Nuclear Materials

10

Computational Thermodynamics of Nuclear Materials

P. S. Ghosh[1,2], K. Ali[1,2] and A. K. Arya*[1,2]

[1]*Glass & Advanced Materials Division, Bhabha Atomic Research Centre (BARC), Trombay – 400085, INDIA*
[2]*Homi Bhabha National Institute, Anushaktinagar, Mumbai – 400094, INDIA*

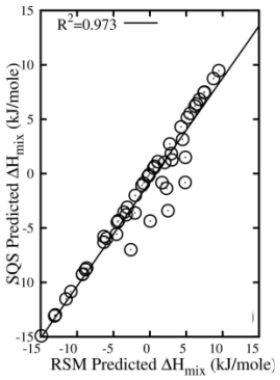

Correlation between the enthalpy values calculated from regular solution model (RSM) and those of the full SQS

ABSTRACT

For improved performance of present generation nuclear reactors and realization of advanced Generation-IV reactors, development of new materials with desired properties is of utmost importance. Design and development of new materials for various stages of nuclear fuel cycle is challenging due to associated radio-toxicity involved in the handling of nuclear fuels for front- and back-end of closed fuel cycle. Computational thermodynamics provides a unique avenue to determine fundamental thermodynamic properties of the nuclear materials in a temperature and composition range which are otherwise not attainable by experiments. High temperature thermodynamic properties are essential to design new materials, to analyse safety aspects and to simulate performance of the materials in reactor operating conditions. The Present article elaborates on three aspects of design and development of new materials using density functional theory (DFT) and classical molecular dynamics (MD) based simulation strategies. Firstly, the study of thermal properties of $U_{1-x}Np_xO_2$/ $Th_{1-x}Np_xO_2$ mixed oxides fuels are presented with an aim to develop thermal property dataset over a wide temperature and composition range. Secondly, design principles of new low-activation high entropy alloys are elaborated with an aim to find new structural material for new generation reactors. Finally, energetics of incorporation/solution of fission metals in Fe-Zr intermetallics is discussed with an aim to profile Fe-Zr alloys as a wasteform for high level nuclear metallic wastes.

KEYWORDS: *Molecular dynamics (MD), Density functional theory (DFT)*

Introduction

Nuclear energy is a clean source of energy and a promising alternative to the fossil fuels. Generation-IV reactors design concepts aim to provide nuclear power facilities that are safer, resistant to proliferation and economically sustainable. The most important factor in the development and implementation of Gen-IV reactors is the dependability and performance of structural materials for both in-core and out-of-core applications [1]. Design and development of new materials for various stages of nuclear fuel cycle is challenging due to associated radiotoxicity. Computational thermodynamics provides a unique avenue to determine fundamental thermodynamic properties of the nuclear materials in a temperature and composition range which are otherwise not attainable by experiments. In this article, we have discussed three studies based on computational thermodynamics, viz., study of thermal properties of mixed-oxide fuels, high throughput screening of single phase high entropy alloys and assessment of Fe-Zr alloys as a host for the high level metallic wastes.

Computational Methods

Classical molecular dynamics (MD) simulations were carried out using Large-scale Atomic Molecular Massively Parallel Simulator (LAMMPS) package to determine thermal properties of $U_{1-x}Np_xO_2$ and $Th_{1-x}Np_xO_2$ systems. The interaction potential between the atoms was modelled by a combination of Buckingham-Morse and many-body potentials. NPT ensemble, using the Nosé-Hoover thermostat and barostat, was used in the MD runs. For calculations of thermal conductivity within LAMMPS, the Green-Kubo formalism was adopted [2]. Nudge elastic band method as implemented in LAMMPS was used to calculate the migration barrier of O vacancies. To capture substantial oxygen diffusion on the limited MD timescale, 1% oxygen vacancies were introduced in the supercell.

Spin-polarized density functional theory (DFT) calculations, as implemented in Vienna Ab-initio Simulation Package [3,4], were employed. The interaction between the atoms were modelled using projector augmented wave (PAW) potentials [5] with generalized gradient approximation (GGA) based exchange-correlations, as parametrized by Perdew, Burke and Enzerhof (PBE) [6]. Optimized k-point mesh and cut-off energy were used for all the calculations. To model disordered alloys, special quasi-random structures (SQS) were generated using Monte Carlo method as implemented in ATAT package [7].

Thermal Properties of Transmutation Fuels

Increasing energy efficiency by recycling the spent fuel along with major actinides Np, Pu and Am is one of the main objectives of future nuclear program. NpO_2 based mixed oxide (MOX) transmutation fuels are specifically important because of their high yield during the burn-up and 106 years of half life [8,9]. Because of the related radio-toxicity of these materials, the impact of adding MAs to MOX on thermal and diffusional characteristics has not been well investigated through experiments. Therefore, thermal and diffusional properties, viz., thermal expansion, thermal conductivity and oxygen diffusivity of NpO_2 based MOX using atomistic simulations [2,10] were evaluated.

*Author for Correspondence: A. K. Arya
E-mail: aarya@barc.gov.in

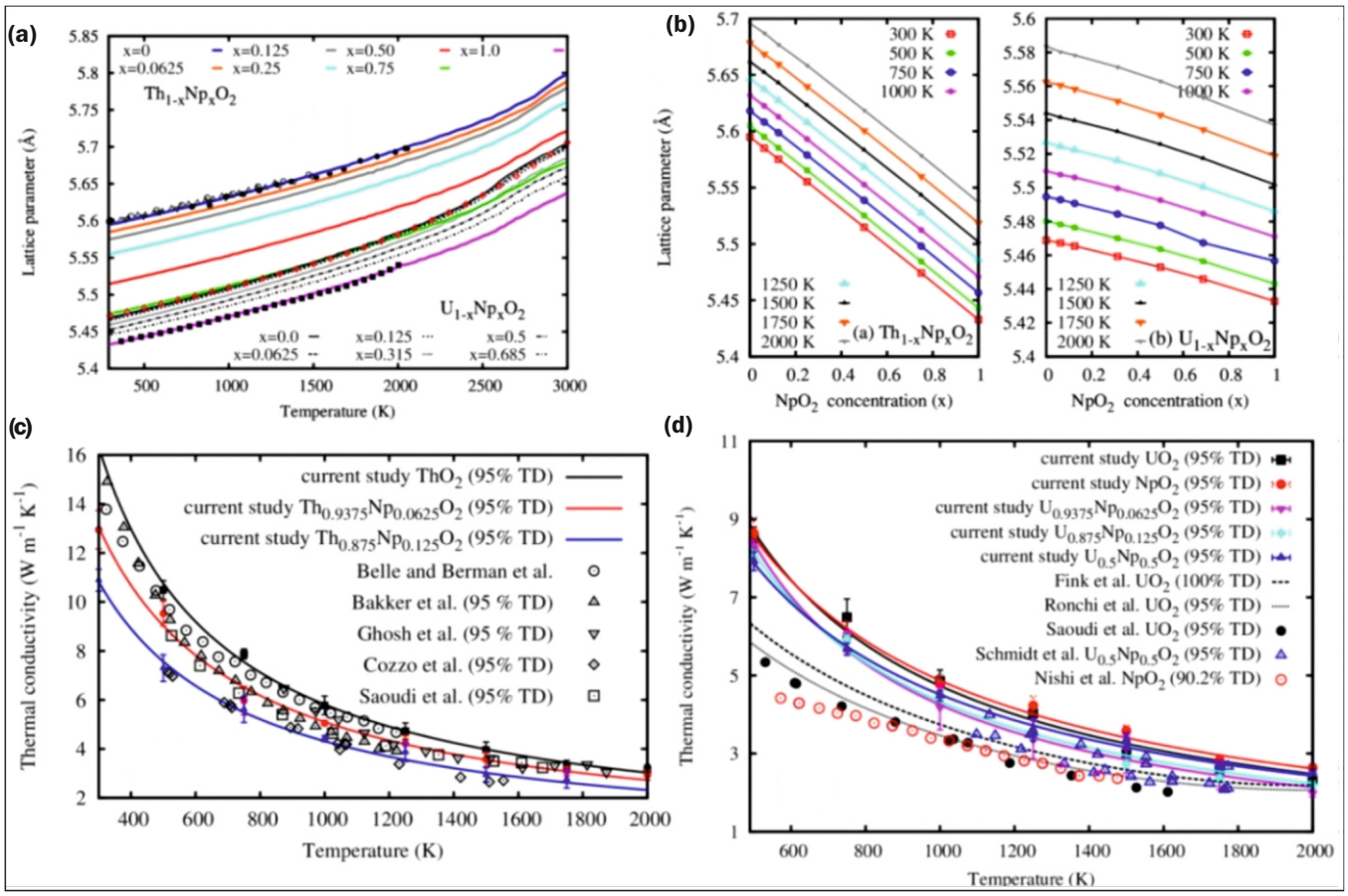

Fig.1: Variation of (a) lattice parameters of $Th_{1-x}Np_xO_2$ and $U_{1-x}Np_xO_2$ (x=0.0, 0.0625, 0.125, 0.25, 0.50, 0.75 and 1.0) as a function of temperature, (b) lattice parameters as a function of NpO_2 concentration. Variation of thermal conductivity of (c) $Th_{1-x}Np_xO_2$ (x=0.0, 0.0625 and 0.125) and (d) $U_{1-x}Np_xO_2$ (x=0.0, 0.0625, 0.125, 0.5 and 1.0) as a function of temperature. Lines present MD calculated values and points present high temperature XRD values.

The lattice parameters of $Th_{1-x}Np_xO_2$ and $U_{1-x}Np_xO$ decrease with temperature at all the studied compositions (see Fig.1 (a)). The overall trend in lattice parameters, which follow Vegard's law, is in good agreement with the experimental results. The lattice parameters of $Th_{1-x}Np_xO_2$ and $U_{1-x}Np_xO_2$ MOX decrease with the NpO_2 content (see Fig.1 (b)). Further, it can be seen from Fig.1 (b) that the rate of decrease in the lattice parameter of $Th_{1-x}Np_xO_2$ is higher than that of $U_{1-x}Np_xO_2$, which suggest that NpO_2 has a greater influence on lattice parameters for $Th_{1-x}Np_xO_2$ than $U_{1-x}Np_xO_2$. This phenomenon can be explained by the differences in ionic sizes of Th^{4+} (1.19 Å), U^{4+} (1.14 Å) and Np^{4+} (1.12 Å) in an 8-fold coordination. Further, the variation of lattice parameters (in Å) of $Th_{1-x}Np_xO_2$ & $U_{1-x}Np_xO_2$ MOX can be presented as a function of NpO_2 concentration (x, $1.0 \geq x \geq 0.0$) and temperature (T, $2000 \geq T \geq 300$):

$$a(Th_{1-x}Np_xO_2) = -0.160777x + 4.44721 \times 10^{-5}T + 6.87589 \times 10^{-9}T^2 + 5.57487$$
$$a(U_{1-x}Np_xO_2) = -0.0397186x + 4.56747 \times 10^{-5}T + 8.35801 \times 10^{-9}T^2 + 5.45702$$

The calculated thermal conductivity (TC) of $Th_{1-x}Np_xO_2$ (x=0.0, 0.0625 and 0.125) and $U_{1-x}Np_xO_2$ (x=0.0, 0.0625, 0.125, 0.5 and 1.0) along with the experimental values of ThO_2, UO_2, NpO_2 and $U_{0.5}Np_{0.5}O_2$ are plotted in Fig.1 (c) and 1 (d). The TC values of UO_2 and NpO_2 are quite close across this temperature range. However, MD calculated TC values of both UO_2 and NpO_2 are grossly overestimated at lower temperature (<1000 K) compared to experimental values (see Fig.2 (d)). In order to improve the accuracy of the thermal-conductivity predictions for UO_2, MD results need to be corrected for the spin-phonon-scattering mechanism by adding the corresponding relaxation time derived from existing experimental data. Fig.2 (d) also indicates a small reduction in TC values for $U_{1-x}Np_xO_2$, even at low temperatures, due to reduction in the phonon mean free path coming from scattering associated with a non-uniform cation sub-lattice. The degradation of the UO_2 TC due to Np substitutional defects is relatively small compared to the addition of Np in ThO_2.The calculated TC values of $Np_{0.5}U_{0.5}O_2$ are lower than those of pure UO_2 and NpO_2 due to higher impurity-phonon scattering at low temperatures (<750K). The calculated TC values of $Np_{0.5}U_{0.5}O_2$ also match the experiments well throughout the temperature range with maximum deviation of 15%. This is consistent with the experimental observation that the TC of NpO_2 with 95% theoretical density (TD) was close to that of $Np_{0.5}U_{0.5}O_2$ above 1098K. At higher temperatures (above 750K), the TC values are almost independent of the NpO2 concentration and the TC values for UO_2, NpO_2 and $U_{1-x}Np_xO_2$ MOX almost superimpose at high temperatures [2].

The mean square deviations (MSD) of pure ThO_2, UO_2, NpO_2 and $Th_{1-x}Np_xO_2$, $U_{1-x}Np_xO_2$ MOX at five intermediate compositions for a temperature range from 750K to 2000K were calculated (Fig.2). The higher slope of MSD for NpO_2 can be attributed to the lower oxygen migration energy (E_m) in NpO_2 than in the ThO_2. By assuming Arrhenius relationship, the D is related to the migration energy (E_m) as $D=D_0 \exp(E_m/k_BT)$, where D_0 is the pre-exponential term, k_B and T is Boltzman constant and temperature, respectively. From the logarithmic plot of D as a function of $1/T$, E_m is determined over the NpO_2 concentration in MOX and those values are shown in Fig.2. Moreover the sequence of the E_m values of the pure oxides is consistent with that determined from NEB calculations. Fig.2

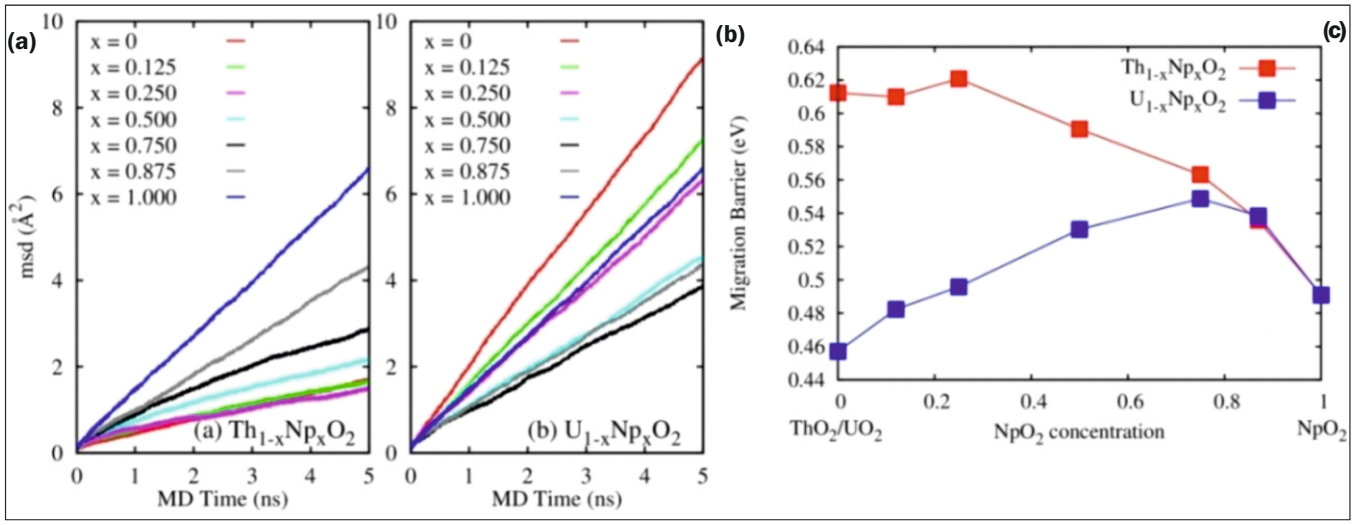

Fig.2: Mean square displacement (MSD) of oxygen as a function of MD simulation time in (a) $Th_{1-x}Np_xO_2$ and (b) $U_{1-x}Np_xO_2$ MOX calculated at 750K. (c) The migration barriers (E_m) of oxygen vacancy in $Th_{1-x}Np_xO_2$ and $U_{1-x}Np_xO_2$ MOX as a function of NpO_2 concentration evaluated from MD calculated oxygen diffusivity as a function of temperature (Arrhenius plot).

shows slight increase of E_m with increase of NpO_2 concentration for $Th_{1-x}NpO_2$ MOX up to x=0.25 followed by continuous decrease up to x=1.0. On the contrary, the E_m increases continuously with increasing NpO_2 concentration up to x=0.75 followed by decreasing trend up to x=1.0. Fig.2 clearly shows nonlinear variation of the E_m with NpO_2 concentration and maxima lies around x=0.25 and 0.75 for $Th_{1-x}NpO_2$ and $U_{1-x}NpO_2$ MOX, respectively.

High throughput screening of High-entropy Alloys

The structural materials of Gen-IV reactors must withstand conditions that are far harsher than what the nuclear power plants of today can handle, including a higher neutron flux, a more corrosive environment and higher operating temperatures. The existing alloys, viz., ferritic/martensitic steels, austenitic stainless steels, nickel-base alloys are not suitable for next generation reactors. High-entropy alloys (HEA), a new class of material, is a promising structural material for Gen-IV reactors. Present article elaborates a design principle of new low-activation single phase HEA using a computational high-throughput screening followed by experimental validations [11,12].

Designing of a HEA with desired properties from a vast composition space only by experimental means is a formidable task. Therefore, computational approaches can be efficiently used to explore this vast composition space. In literature, there are a number of empirical models [see ref. 12] which were proposed to predict the formation of single phase HEA. The precise value of mixing enthalpy (ΔH_{mix}) for a HEA holds significant importance, as it serves as a crucial parameter in all the empirical models. The ΔH_{mix} can be calculated using Miedama model which is quick but not accurate. On the other hand DFT calculations using SQS can be employed to calculate the ΔH_{mix}, which is accurate but time consuming (as we need big supercell to handle the configurational disorder of the system). The following method was employed in this study to calculate the mixing enthalpy of the HEAs:

(I) ΔH_{mix} of all the binary alloys (AB solid solutions) formed by the low activation elements (Ti, V, Cr, Mn, Fe, Ta, and W) have been calculated at 3 different compositions, viz., 25:75, 50:50 and 75:25, using 32 atom-SQS. (ii) using the binary ΔH_{mix}, the interaction parameters of the binary combinations are calculated by using a regular solution model (RSM) $\Delta H_{mix}^{ij} = \sum_{i=1,j>i}^{No.of elements} \Omega_{ij} c_i c_j$, where Ω_{ij} and $c_{i(j)}$ are the interaction parameter between i and j atoms and concentration of i(j) atom. (iii) Ω_{ij} values are used to calculate the ΔH_{mix} of ternary, quaternary and quinary alloys. To check the accuracy of the above methodology, we have compared the ΔH_{mix} of few ternary, quaternary and quinary alloys calculated using the above mentioned RSM to the ΔH_{mix} computed using bigger SQS cell. It has been found that accuracy of ΔH_{mix} of RSM is similar to the SQS cell method (R^2 value of 0.973) leading to conclusion that the ΔH_{mix} calculated using RSM enough for calculating the ΔH_{mix} of HEAs (Fig.3 (a)).

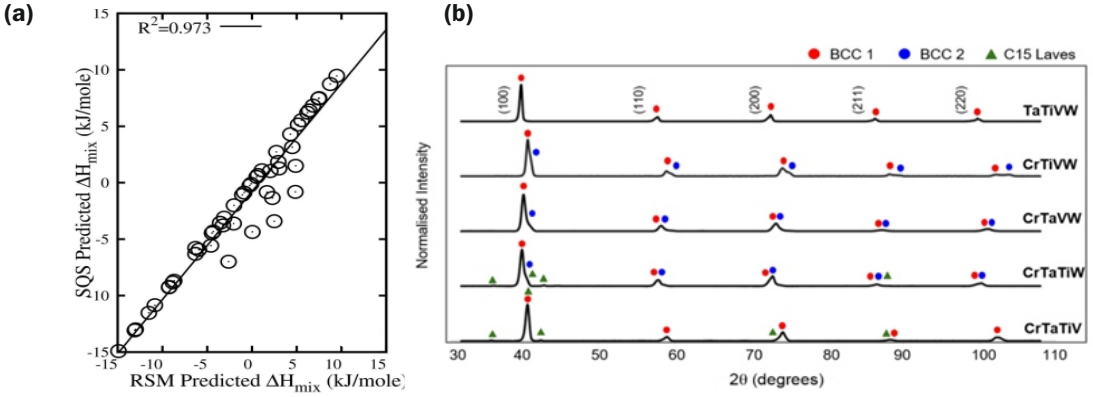

Fig.3: (a) Correlation between the enthalpy values calculated from regular solution model (RSM) and those of the full SQS and (b) XRD pattern of high-entropy alloys.

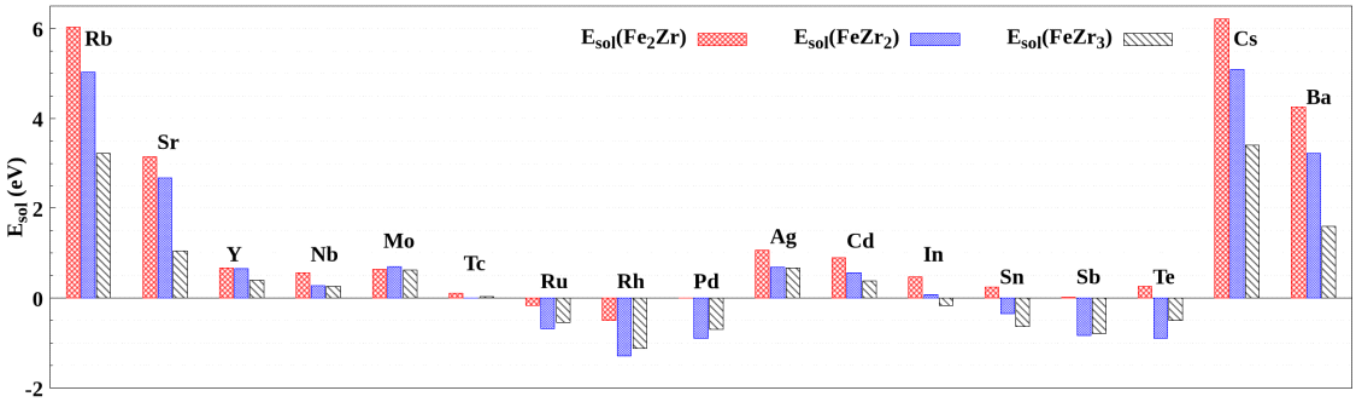

Fig.4: Solution energies of the s-, p- and d-block FMs in c-Fe_2Zr, t-$FeZr_2$ and o-$FeZr_3$ intermetallics.

In the literature, 8 different empirical models (details are in Ghosh et al. [12]) are available, which are used to predict the formation of single phase HEA. But it is important to mention that not a single parameter is 100% fail-safe in this prediction. Therefore, bench-marking of all the models have been carried out against the experimentally reported 36 distinct quaternary/quinary as-cast HEAs from the palette of seven low-activation elements. It has been found that the model proposed by Ye et al. [13] is the most suitable in our alloy palette, therefore, further predictions were made using the same model. We have predicted the probability of single phase formation in all the 35 and 21 equiatomic quaternary and quinary alloys, respectively. To validate our predictions, experimental studies are carried out on 5 near-equiatomic alloys, viz., TaTiVW, CrTiVW, CrTaVW, CrTaTiW and CrTaTiV. Experimental studies suggest that TaTiVW, CrTiVW and CrTaVW alloys do form single/two bcc phase; while CrTaTiW and CrTaTiV alloys form bcc+Laves phase (Fig.3 (b)). These observations are in very good agreement with our predictions.

Fe-Zr Alloys as Host Matrices for High Level Nuclear Metallic Waste

The growth of the nuclear power industry is also contingent upon the efficient management of nuclear wastes. While there is proper wasteforms available for immobilizing high-level (radioactivity>$3.7x10^{11}$Bq/L) liquid waste, a suitable wasteform for the immobilization of high-level metallic wastes, viz., hulls, grids, spacers, etc., generated from reactors, remains lacking. Experimental findings have identified stainless steel (SS) and Zirconium (Zr) based alloys, such as SS-15wt% Zr, Zr-16wt% SS, and Zr-8wt% SS, as promising materials for metallic wasteform [14]. Notably, Fe-Zr intermetallic phases, viz., (c)ubic-Fe2Zr, (t)etragonal-$FeZr_2$, and (o)rthorhombic-$FeZr_3$, are predominant in SS-Zr alloys and play a crucial role in accommodating actinides present in metallic wastes [15]. In view of these considerations, our study explores the potential of Fe-Zrintermetallics to function as a wasteform for fission metals (FMs).

The thermodynamical, mechanical as well as dynamical stability of c-Fe_2Zr, t-$FeZr_2$ and o-$FeZr_3$ phases were first established from their formation energy, single crystal elastic constants and phonon dispersions [16]. Further, to study the feasibility of incorporation of the s-, p- and d-block FMs, viz., Rb, Sr, Cs, Ba, In, Sn, Sb, Te, Y, Nb, Mo, Tc, Ru, Rh, Pd, Ag and Cd in the Fe-Zrintermetallics, we have calculated the incorporation and solution energy of the FMs in c-Fe_2Zr, t-$FeZr_2$ and o-$FeZr_3$ intermetallics [16-18]. The calculated incorporation energies of the FMs suggest that the incorporation of all the FMs, except Rb and Cs, is exothermic in nature. The incorporation of Rb and Cs in all the three intermetallics is endothermic, which indicates that they are difficult to incorporate in these intermetallics. Interestingly, it is also observed that the Zr-rich intermetallics (t-$FeZr_2$ and o-$FeZr_3$) are energetically more preferred as hosts for all the FMs, except Tc, Ru and Rh atoms as compared to Fe-rich c-Fe_2Zr owing to their larger negative incorporation energies.

However, it has been found that the vacancy formation energy of Fe/Zr in all the intermetallics are greater than 1 eV, which suggest that the equilibrium concentration of vacancy is very low in the system. Therefore, solution energies are more appropriate to assess the potential of these intermetallics to incorporate the fission metals. The calculated lowest solution energies (E_{sol}) of *s-*, *p-* and *d*-block FMs in the c-Fe_2Zr, t-$FeZr_2$ and o-$FeZr_3$ intermetallics are shown in Fig.4. At first, the site preferences of the FMs were determined based on their solution energies at the Fe and Zr sites. It has been found that s-block FMs, In, Sn, Y, Nb, Mo, Ag and Cd prefer to occupy Zr site; while the remaining FMs, viz., Tc, Ru, Rh, Pd, Sb and Te prefer to occupy Fe site. The calculated E_{sol} of s-block FMs are higher than 1 eV suggesting that the s-block FMs can be easily segregated from the intermetallics. The solution energies of p- and d-block FMs in the three intermetallics are 0.5 and 1.0 eV, respectively, possibly making them soluble at higher temperatures due to lattice modulations. Overall, the solution energies of the FMs in the t-$FeZr_2$ and o-$FeZr_3$ phases are less than those in the c-Fe_2Zr phase except for the Mo atom which has almost equal solution energy in the three intermetallics.

Conclusions

The Present study elaborates on the usage of computational thermodynamics to determine fundamental thermodynamic properties of nuclear materials in a temperature and composition domain which are otherwise not attainable by experiments alone. Major conclusions arrived at are as follows:

(I)A database of thermal expansion, thermal conductivity and oxygen diffusion parameters has been developed for Np-based transmutation fuels which can be used to design new generation fuels, to analyse safety aspects and to simulate performance of the materials in reactor operating conditions.

(ii) The Occurrence of new single-phase high-entropy alloys and composition ranges are determined where they remain in single-phase. Further mechanical and defect properties of those alloys are ongoing with an aim to develop ductile radiation-resistant HEAs.

(iii) Fe-Zr alloys are suitable for the incorporation of p- and d- block fission elements with limited solubility.

(iv) We believe that limited experimental efforts are required to validate some of our predictions.

References

[1] Yvon, Pascal, ed. Structural materials for generation IV nuclear reactors. Woodhead Publishing, 2016.

[2] P.S. Ghosh, A. Arya, N. Kuganathan, R.W. Grimes, Thermal and diffusional properties of $(Th,Np)O_2$ and $(U,Np)O_2$ mixed oxides, Journal of Nuclear Materials, 521, 2019, 89-98.

[3] G. Kresse, J. Furthmuller, Efficiency of ab-initio total energy calculations for metals and semiconductors using a plane-wave basis set, Computational materials science 6 (1996) 15–50.

[4] G. Kresse, J. Furthmuller, Efficient iterative schemes for ab initio total-energy calculations using a plane-wave basis set, Physical Review B 54 (1996) 11169–11186.

[5] P.E. Blöchl, Projector augmented-wave method, Phys. Rev. B 50 (1994) 17953–17979.

[6] J.P. Perdew, K. Burke, M. Ernzerhof, Generalized Gradient Approximation Made Simple, Phys. Rev. Lett. 77 (1996) 865–3868.

[7] A. van de Walle, M. Asta, G. Ceder, The alloy theoretic automated toolkit: A user guide, Calphad 26 (2002) 539.

[8] Actinide and fission product partitioning and transmutation, Status and assessment report, NEA, OECD, 1999.

[9] Bhatti, Zaki, Hyland, B., and Edwards, G. W.R. Minor actinide transmutation in thorium and uranium matrices in heavy water moderated reactors. United States: American Nuclear Society, 2013.

[10] Phase stability, electronic structures and elastic properties of $(U,Np)O_2$ and $(Th,Np)O_2$ mixed oxides, P.S. Ghosh, N. Kuganathan, A. Arya and R.W. Grimes,) Phys. Chem. Chem. Phys., 2018, 20, 18707-18717.

[11] Liangzhi Tan, Kawsar Ali, Partha Sarathi Ghosh, Ashok Arya, Ying Zhou, Roger Smith, Pooja Goddard, Dhinisa Patel, Hamed Shahmir, Amy Gandy, Design principles of low-activation high entropy alloys, Journal of Alloys and Compounds, 907, 2022, 164526.

[12] P.S. Ghosh, K. Ali, A. Arya, Efficient screening of single phase forming low-activation high entropy alloys, Journal of Alloys and Compounds, 978, 2024, 173172.

[13] Y. Ye, Q. Wang, J. Lu, C. Liu, Y. Yang, Design of high entropy alloys: A single-parameter thermodynamic rule, Scripta Materialia 104 (2015) 53.

[14] S.M. McDeavitt, D. P. Abraham, J.Y. Park, Evaluation of stainless steel–zirconium alloys as high-level nuclear waste forms, Journal of Nuclear Materials, 257, 1998, 21.

[15] D.P. Abraham, N Dietz, Role of laves intermetallics in nuclear waste disposal, Materials Science and Engineering: A, 329-331, 2002, 610-615.

[16] Kawsar Ali, A. Arya, P.S. Ghosh, G.K. Dey, A first principles study of cohesive, elastic and electronic properties of binary Fe-Zr intermetallics, Computational Materials Science, 112, 2016, 52.

[17] Kawsar Ali, A. Arya, Structural and electronic properties of Fe-Zr intermetallics incorporating s-, p- and d-block fission metals, Journal of Nuclear Materials, 558, 2022, 153389

[18] Kawsar Ali, A. Arya, Cohesive, elastic and anisotropic properties of s-, p- and d-block fission metals substituted Fe-Zr intermetallics, Progress in Nuclear Energy, 168, 2024, 105025.